

In Vivo and *In Vitro* Comparison of the Charge Injection Capacity of Platinum Macroelectrodes

Ronald T. Leung, Mohit N. Shivdasani, David A. X. Nayagam*, *Member, IEEE*,
and Robert K. Shepherd, *Member, IEEE*

Abstract—Platinum (Pt) is the most commonly used metal for stimulating electrodes. This study aims to determine the amount of charge that can be delivered without causing irreversible electrochemical reactions (charge injection capacity, Q_{inj}) of Pt macroelectrodes (geometric surface area $>0.001\text{ cm}^2$) *in vitro* and *in vivo* using voltage transient measurements. Pt macroelectrodes were stimulated with biphasic charge-balanced cathodic-first constant-current pulses in phosphate buffered saline. Potential excursions were measured (versus Ag/AgCl electrode) and used to determine Q_{inj} . The *in vitro* Q_{inj} were compared to those measured *in vivo* following: acute and chronic implantation close to the retina; chronic intracochlear implantation; and acute subdural implantation, in the cat. Q_{inj} increased with pulsewidth from 35 to 54 $\mu\text{C}/\text{cm}^2$ for respective pulse widths of 100 to 3200 μs per phase *in vitro*. Q_{inj} was significantly less *in vivo*. There was no significant difference in Q_{inj} between acutely (3.84 to 16.6 $\mu\text{C}/\text{cm}^2$ with pulsewidths of 100 to 3200 μs) and chronically (6.99 to 15.8 $\mu\text{C}/\text{cm}^2$ with pulsewidths of 200 to 3200 μs) implanted suprachoroidal electrodes. Intracochlear Q_{inj} was not different to suprachoroidal Q_{inj} , while subdural Q_{inj} was significantly less than the suprachoroidal Q_{inj} ($p < 0.05$). These results have important implications in providing guidelines on Q_{inj} for the safe use of Pt stimulating macroelectrodes and question the relevance of measuring Q_{inj} *in vivo* using voltage transients.

Index Terms—Electrical stimulation, electrochemical processes, implantable devices, neural and visual prosthesis, platinum electrodes.

I. INTRODUCTION

PLATINUM (Pt) is a noble metal that is commonly used as a stimulating electrode material for neural prostheses. It has been widely used clinically in cochlear implants [1], [2], retinal prostheses [3]–[5], cortical implants [6]–[11], and for other experimental purposes [9]–[18]. Generally, charge injection into neural tissue is achieved through a combination of several electrochemical reactions at the electrode-tissue interface. These include capacitive double-layer charging, reversible Faradaic reactions, and irreversible Faradaic reactions [19]–[21]. The first

two mechanisms can inject charge without producing harmful electrochemical products, while the latter method can cause damage to surrounding tissues and to the stimulating electrode itself [19]. Electrolysis of water is one type of irreversible Faradaic reaction of particular concern since it can lead to localized pH changes [20], [22], and the evolution of gases could physically displace tissue [20]. Electrolysis of water can be avoided by ensuring that the maximum cathodic (E_{mc}) and anodic potentials on the electrode, during electrical stimulation stay within the “water window” [−0.6 to 0.9 V versus Ag/AgCl for Pt electrodes in phosphate buffered saline (PBS)] [23], [24]. The amount of charge per unit area that can be delivered through an electrode without causing water electrolysis is known as the charge injection capacity (Q_{inj}). Dissolution of Pt is also irreversible and is a concern, as it can lead to the formation and release of toxic products [25].

Q_{inj} can be measured using voltage transients [23], [26], [27] and is a function of several variables. It is dependent on the geometry of the electrode with smaller electrodes tending to have larger Q_{inj} [21]. Also, the charge density on nonspherical electrodes will be nonuniform with charge accumulating near the edges or other sharp points, especially during phases such as the stimulus pulse onset [28], [29]. Q_{inj} has been found to increase with pulsewidth when measured *in vitro* and is dependent on the conductivity and composition of the conducting media and temperature [21], [30].

A reduction of *in vivo* Q_{inj} compared to *in vitro* Q_{inj} has been observed in acutely and chronically implanted electrodes with materials such as iridium oxide [31], [32], but this has not been investigated using Pt electrodes. Biological media is different to PBS since it contains many different electrolytes and organic molecules. A decrease in ionic conductivity or obstruction to the diffusion of counter ions can lead to a decrease of Q_{inj} *in vivo* [27]. Adsorption of proteins can inhibit Pt oxidation and oxide reduction [33], [34]. The concentration of oxygen in the physiological environment is lower than in PBS, and this limits the contribution of oxygen reduction to Q_{inj} *in vivo* [33], [35]. Additionally, chronically implanted electrodes may evoke a tissue response resulting in fibrosis, further altering the electrode-tissue interface and affecting Q_{inj} .

Several groups have estimated the electrochemical Q_{inj} of Pt *in vitro*, with the consensus that 100 to 150 $\mu\text{C}/\text{cm}^2$ can be delivered with 200 μs pulses [23], and that the maximum charge that can be delivered by exhausting all reversible charge injection mechanisms is 420 to 490 $\mu\text{C}/\text{cm}^2$ [36] for Pt macroelectrodes (defined as electrodes with geometric surface area greater than 0.001 cm^2). Other groups have reported Q_{inj} in the range of 80 to 120 $\mu\text{C}/\text{cm}^2$ [37]. Fine Pt powder (Pt black) can be

Manuscript received December 19, 2012; revised November 6, 2013, December 18, 2013, June 12, 2014, and September 10, 2014; accepted October 26, 2014. Date of publication November 3, 2014; date of current version February 16, 2015. This work was supported by the Australian Research Council through its Special Research Initiative in Bionic Vision Science and Technology grant to Bionic Vision Australia. The work of R. T. Leung was supported by the Harold Mitchell Foundation. *Asterisk indicates corresponding author.*

R. T. Leung, M. N. Shivdasani, and R. K. Shepherd are with the Bionics Institute, East Melbourne, Vic. 3002, Australia, and also with The University of Melbourne, Parkville, Vic. 3010, Australia (e-mail: rleung@bionicsinstitute.org; mshivdasani@bionicsinstitute.org; rshepherd@bionicsinstitute.org).

*D. A. X. Nayagam is with the Bionics Institute, East Melbourne, Vic. 3002, Australia, and also with The University of Melbourne, Parkville, Vic. 3010, Australia (e-mail: dnayagam@bionicsinstitute.org).

Digital Object Identifier 10.1109/TBME.2014.2366514

electroplated onto Pt electrodes to enhance the real surface area [38] and this can increase Q_{inj} [38], [39]. The real surface area of Pt can also be increased by laser roughening [39], [40] which increases Q_{inj} ; however, the surface charge density will be less uniform. Conversely, the real surface area can be decreased by polishing the electrode, resulting in a decreased Q_{inj} [23]. In this paper, surface area always refers to the geometric surface area unless specified otherwise, and references to charge density and pulsewidth refer to the charge density or pulsewidth per phase, respectively. The real surface area of smooth Pt foil is typically 1.4 times the geometric surface area [33], [41].

Since Q_{inj} is dependent on a large number of variables, Q_{inj} should be determined for each application with a method that closely mimics the conditions of the intended use. Our group has developed a retinal prosthesis which is undergoing clinical trials (NCT01603576). It uses disk-shaped Pt macroelectrodes implanted in the suprachoroidal space behind the retina [42]. As different stimulation paradigms are investigated, a broad range of stimulation parameters are likely to be used clinically. For example, perceptual responses to stimulation with long pulsewidths may be investigated since it is well known that increasing the duration of the pulsewidth decreases the current required to reach threshold [4], [43]–[47]. A decrease in current threshold would therefore allow stimulators with lower compliance voltage to be used. In the interests of patient safety, it is vital to have boundaries on electrochemically safe stimulation parameters based on the Q_{inj} , which can guide clinicians and psychophysics investigators.

The *in vitro* Q_{inj} limits of Pt determined by various groups [23], [33], [36], [40] are commonly used as safety guidelines *in vivo* although the effect of the differences in electrode geometry, pulsewidth, and the physiological environment on Q_{inj} have not been fully appreciated [48]–[54]. Similarly, the electrodes in our retinal prosthesis design have different geometries to these prior studies, and the pulsewidths proposed for clinical use are greater than those previously investigated. Additionally, we are not aware of any studies where a systematic evaluation of Q_{inj} for Pt electrodes *in vivo* has been performed. This study investigated the theoretical limits of Q_{inj} in Pt macroelectrodes with a range of clinically relevant pulsewidths using voltage transient measurements. The Q_{inj} of Pt was determined *in vitro* and *in vivo* in a retinal prosthesis model following both acute and chronic implantation in the suprachoroidal space of the eye. The results obtained from acute suprachoroidal implantation were additionally compared to the Q_{inj} of subdural electrodes, while the chronic suprachoroidal results were compared to the Q_{inj} measured in a chronically implanted intracochlear array, as both subdural and cochlea prostheses employ Pt macroelectrodes.

II. METHOD

A. Electrode Preparation

Electrode arrays were fabricated in a similar fashion to the clinical suprachoroidal retinal prostheses being developed by our group [55], [56]. Insulated Pt-Ir wire (90%:10%) was welded to 700- μm -diameter Pt disks punched from 0.05-mm-

thick smooth Pt foil (purity 99.95%, Goodfellow Cambridge, U.K.). Disks were placed into a thin silicone sheet cast in-house with 700- μm -diameter perforations. 50 μm of the outer edge was covered by the silicone sheet resulting in an exposed geometric area of $2.83 \times 10^{-3} \text{ cm}^2$ with a recess of 50 μm . The Pt wires, weld joints, and one face of the Pt disks were sealed in silicone [see Fig. 1(a)]. Prior to each stimulation experiment, electrode arrays were cleaned by ultrasonication for 10 min in detergent (Pyroneg, Diversey Australia, NSW, Australia), twice for 5 min in double distilled water, 5 min in 96% ethanol, 15 min in isopropyl alcohol, 5 min in 96% ethanol, and twice more for 5 min in double distilled water. For *in vivo* studies electrode arrays were also steam sterilized. Two similarly manufactured arrays with two disk electrodes each were used for a subdural implantation study.

A commercially manufactured Hybrid L14 (Cochlear Ltd., NSW, Australia) electrode array was used for intracochlear implantation [1]. The exposed geometric surface area of the intracochlear electrodes selected for this study was between 2.0×10^{-3} and $2.3 \times 10^{-3} \text{ cm}^2$.

B. Surgical Procedures

All animals were treated in accordance with the requirements of the Royal Victorian Eye and Ear Hospital Animal Research and Ethics Committee (Ethics Approval #10/206AB), the “Australian code of practice for the care and use of animals for scientific purposes” (2004), and the Prevention of Cruelty to Animals Act 1986 and amendments. Suprachoroidal electrode implantation procedures were performed at the Royal Victorian Eye and Ear Hospital by vitreoretinal surgeons based on previously published methods [55]. Briefly, healthy young adult felines were anesthetized with xylazine (Troy Laboratories, Australia, 2 mg/kg) and ketamine (Troy Laboratories, Australia, 20 mg/kg) subcutaneously. Surgical anaesthesia was maintained with gaseous isoflurane (1% to 3%) in animals with chronic implants ($n = 2$) and intravenous sodium pentobarbital (Troy Laboratories, Australia, 10 to 30 mg/hr) for acute studies ($n = 1$). Intravenous sodium pentobarbital was used during stimulation. A lateral canthotomy was performed followed by a temporal peritomy. A scleral wound was created parallel and 5-mm posterior to the limbus. A suprachoroidal pocket was dissected and the electrode array inserted to a position near the area centralis. The wound was repaired by sutures. Acute suprachoroidal stimulation was performed on one animal from 1 to 72 h after implantation ($n = 18$ electrodes). Suprachoroidal stimulation was also performed on two other animals after a total implantation period of three months ($n = 10$ electrodes).

For the subdural implantation study, a craniotomy was performed over the striate cortex and a small flap in the dura was created. Two small electrode arrays, each with two disk electrodes, were inserted under the dura through the flap with the disks facing the cortex. Cortical stimulation was performed in one animal up to 2 h after implantation ($n = 4$ electrodes).

A separate animal was implanted with an intracochlear electrode array using the method described by Fallon *et al.* [57]. Stimulation was performed six months after implantation ($n = 3$

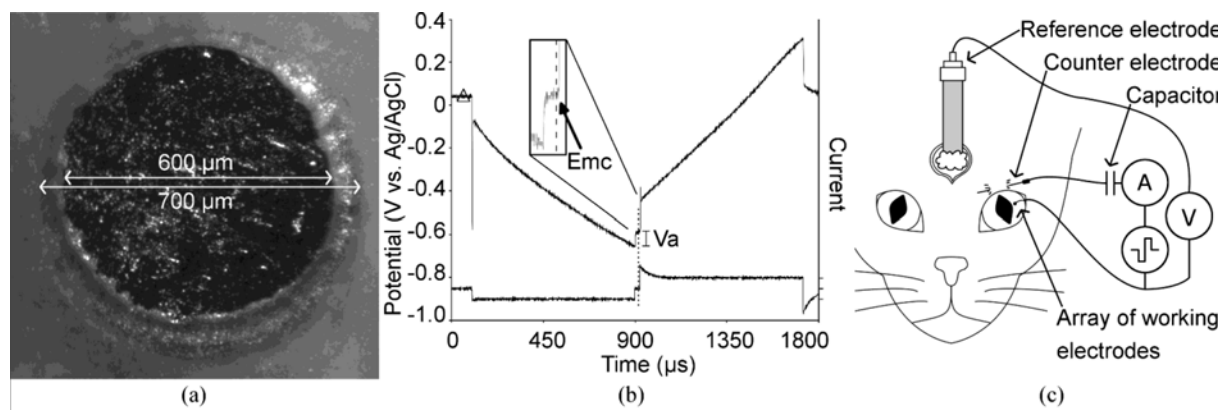


Fig. 1. (a) Typical 700- μm -diameter Pt disk working electrode with an exposed diameter of 600 μm encased in silicone. (b) Representative potential transient (upper trace) and current pulse (lower trace, 125 $\mu\text{A}/\text{div}$) of an 800 μs cathodic-first pulse with a 25 μs interphase gap *in vitro*. E_{mc} can be measured by subtracting the access voltage (V_a) from the maximum negative potential or by measuring the potential near the end of the interphase gap, 20 μs after the cathodic phase offset (dotted line; in this example $E_{mc} = -0.6$ V relative to the Ag/AgCl reference electrode). The interpulse potential can also be measured (triangle). (c) Diagrammatic representation of the *in vivo* potential transient measurement system. Arrays of working electrodes were implanted into felines and stimulated against a capacitively coupled (10 μF) Pt counter electrode. A Ag/AgCl reference electrode was connected to the skull with a salt bridge. The current and voltage waveforms were measured periodically. In this example, the suprachoroidal potential transient measurement system is shown.

electrodes). Animals were overdosed with sodium pentobarbital (150 mg) at the conclusion of experiments.

C. Stimulation Protocol

One disk electrode, not used for potential transient measurements, was selected for cyclic voltammetry (CV) to verify the cleanliness of the electrode fabrication method and confirm the range of the water window. The active electrode was cycled between -0.6 and 1.2 V (versus. Ag/AgCl in 3 M KCl, CH instruments, USA) with a sweep rate of 50 mV/s (EA163, eDAQ, Australia). CV was performed in PBS (0.1 M phosphate buffer, 0.13-M NaCl, pH 7.4), and then in the suprachoroidal space following acute implantation. The water window was determined by analyzing features of the CV waveform [58].

To determine Q_{inj} , electrodes were stimulated with constant-current biphasic cathodic-first charge-balanced capacitively-coupled (10 μF) pulses against a large Pt wire or needle counter electrode using an in-house custom-built stimulator. In addition, the stimulating and return electrodes were shorted at the end of each pulse and remained shorted until the next pulse, to ensure less than 100 nA net direct current and minimal irreversible reactions [59]. The interphase gap was 25 μs during which the electrodes were open circuit. Pulswidths ranged from 100 to 3200 μs . The waveforms of five pulses of the stimulation current and the working electrode potential (versus. Ag/AgCl) were recorded (PXI-4072, National Instruments, USA) after the voltage transient had reached steady state.

E_{mc} can be measured by subtracting the access voltage from the most negative potential of the voltage waveform [see Fig. 1(b)]. However, distinguishing the access voltage from the interface polarization was found to be difficult *in vivo*. Thus, we used a more robust approach in which E_{mc} was measured as the potential near the end of the interphase gap, 20 μs after the end of the cathodic phase [35], [60]. It is important to note that the measured working electrode potential lags the actual

working electrode potential, and that following the sudden voltage change at the cathodic phase offset, the measured working electrode potential exponentially approaches the actual potential. The time constant is greater in environments with significant permittivity, such as *in vivo*. By measuring E_{mc} with a 20 μs delay after the cathodic phase offset, the difference in the measured and actual E_{mc} is minimized. Measuring E_{mc} using the potential near the end of the interphase gap or by subtracting the access voltage from the most negative potential produced similar results *in vitro*.

A salt bridge on the surface of the exposed skull was used to connect the Ag/AgCl reference electrode *in vivo* [see Fig. 1(c)]. Moving the position of the reference electrode to different areas of the animal *in vivo* had minimal effect on the measured E_{mc} . The use of Ag/AgCl reference electrodes *in vivo* to measure the working electrode potential has previously been described [32], [60]. Note that the effect of distance between working microelectrodes and the reference electrode has minimal effect on measurements (personal communication).

Charge injection can cause tissue damage in several ways. Physiologically safe stimulation must operate within the water window. In the present study, Q_{inj} is defined as the charge density that causes the working electrode potential to reach the water window limits. This is a widely accepted method of measuring Q_{inj} *in vitro* [23], [30], [35], [37], [40], [61]–[65] or *in vivo* [27], [32], [60], [66]. In the present study, each electrode was stimulated with a current amplitude that was empirically determined for each pulswidth such that E_{mc} was approximately -0.6 V (the lower limit of the water window). The corresponding charge density was recorded as Q_{inj} . The pulse rate was chosen such that the interpulse potential did not deviate by more than 100 mV from the open-circuit potential. This was 4 pulses/s *in vitro*, and 100 pulses/s *in vivo*. Electrodes were stimulated for 15 min, and waveforms were measured every 5 min *in vivo* to ensure that the electrode voltage waveform had reached a steady state. Because stimulus induced electrode corrosion is more apparent

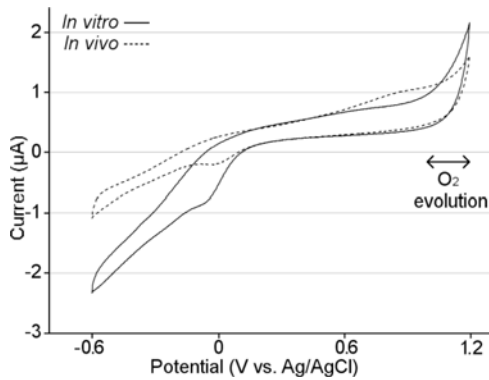


Fig. 2. CVs of a Pt electrode performed in air-saturated PBS and implanted in the suprachoroidal space with a sweep rate of 50 mV/s. Hydrogen evolution did not occur at potentials more positive than -0.6 V. The sudden increase in current at potentials more positive than 0.9 V indicates oxygen evolution.

in vitro [68], electrodes were only stimulated for 5 min, and waveforms were measured every minute *in vitro*. Waveforms typically stabilized within seconds of stimulation. For *in vitro* testing, electrodes ($n = 7$) were tested in PBS maintained at 37 °C. Disk electrode arrays were soaked in PBS prior to *in vitro* stimulation and inspected to ensure that no air bubbles adhered to the electrode array surface.

The *in vitro* Q_{inj} at different pulsewidths were compared with a one-way analysis of variance with the Bonferroni correction. *In vitro* Q_{inj} was compared with the *in vivo* Q_{inj} . Differences in chronic and acute suprachoroidal Q_{inj} were tested with a two-way analysis of variance. Intracochlear and subdural electrodes were stimulated only using a $400\text{-}\mu\text{s}$ pulsewidth and the Q_{inj} was compared with the suprachoroidal Q_{inj} . Differences between suprachoroidal, intracochlear, and subdural Q_{inj} were tested with a one-way analysis of variance.

III. RESULTS

CV tests using our Pt electrodes showed that water electrolysis did not occur at potentials between -0.6 and 0.9 V *in vivo* and *in vitro* [see Fig. 2]. The *in vitro* CV current was more negative at potentials less than 0.15 V, presumably due to the reduction of oxygen.

Potential transients were recorded [see Fig. 3] and used to determine Q_{inj} . There was negligible variation between measurements taken after 1 and 5 min of pulsing *in vitro* and also between measurements taken 5 and 15 min of pulsing *in vivo*. Q_{inj} increased with pulsewidth and, *in vitro*, was 34 to $54\ \mu\text{C}/\text{cm}^2$ with 100 to $3200\text{-}\mu\text{s}$ pulsewidths ($n = 7$) [see Fig. 4]. The Q_{inj} of $3200\text{-}\mu\text{s}$ pulses were significantly different to all other pulsewidths, $1600\ \mu\text{s}$ pulses were different to all other pulsewidths except for $800\ \mu\text{s}$ pulses, and $800\ \mu\text{s}$ pulses were different to $100\ \mu\text{s}$ pulses (one-way analysis of variance, $p < 0.05$). The interpulse potential (potential of the working electrode between pulses) was 89 ± 6 mV (mean \pm standard error; $n = 41$). The maximum anodic potential did not exceed 0.9 V in any case.

The suprachoroidal Q_{inj} *in vivo* was significantly less than the Q_{inj} determined *in vitro* [see Figs. 3, 4]. The mean

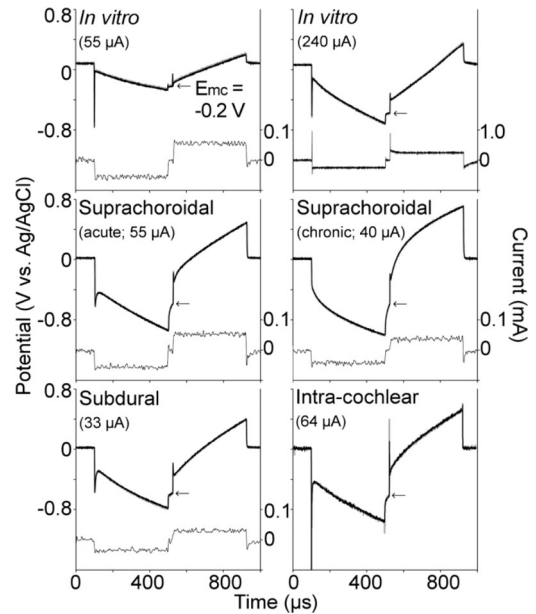


Fig. 3. Voltage excursion and current waveforms of $400\ \mu\text{s}$ pulses *in vitro*, acutely implanted in the suprachoroidal space, chronically implanted in the suprachoroidal space, acutely implanted subdurally and chronically implanted in the cochlea. Measurements taken after 1 min (gray) and 5 min (black) of pulsing *in vitro* and 5 min (gray) and 15 min (black) of pulsing *in vivo* are shown. E_{mc} is -0.6 V as indicated by arrows unless labeled otherwise. Current waveforms were not recorded during intracochlear stimulation. Each panel was recorded using a different electrode. Note the black and gray waveforms are overlaid for most of the plots.

suprachoroidal Q_{inj} *in vivo* was between 8.7 times less ($200\text{-}\mu\text{s}$ pulsewidth) and 3.2 times less ($3200\text{-}\mu\text{s}$ pulsewidth) than that measured *in vitro*. These factors were determined by dividing the *in vitro* Q_{inj} by the mean *in vivo* Q_{inj} at the respective pulsewidths. The mean suprachoroidal Q_{inj} in the acutely implanted animals was between 3.84 to $16.6\ \mu\text{C}/\text{cm}^2$ for pulsewidths of 100 to $3200\ \mu\text{s}$ ($n = 18$). In chronically implanted animals, suprachoroidal Q_{inj} was between 6.99 to $15.8\ \mu\text{C}/\text{cm}^2$ for pulsewidths of 200 to $3200\ \mu\text{s}$ ($n = 10$). There was no difference between acute and chronic suprachoroidal Q_{inj} but there was a significant difference between all pulsewidths (two-way analysis of variance, $p < 0.05$).

With a pulsewidth of $400\ \mu\text{s}$, the mean (\pm standard error) intracochlear Q_{inj} was $10.8 \pm 0.5\ \mu\text{C}/\text{cm}^2$ ($n = 3$) [see Figs. 3, 4]. This was not significantly different to the Q_{inj} of chronically implanted suprachoroidal electrodes with a $400\text{-}\mu\text{s}$ pulse. The mean (\pm standard error) cortical Q_{inj} was $4.63 \pm 0.04\ \mu\text{C}/\text{cm}^2$ ($n = 4$) with a pulsewidth of $400\ \mu\text{s}$, which is significantly less than the Q_{inj} of acutely implanted electrodes in the suprachoroidal space (one-way analysis of variance, $p = 0.002$). The cortical Q_{inj} was also significantly less than the intracochlear Q_{inj} ($p = 0.001$).

IV. DISCUSSION

We have determined the electrochemical Q_{inj} for Pt using pulsewidths between 200 and $3200\ \mu\text{s}$ by measuring the charge density when E_{mc} was at the lower limit of the water window (-0.6 V). The results demonstrated that the *in vitro* Q_{inj} was up

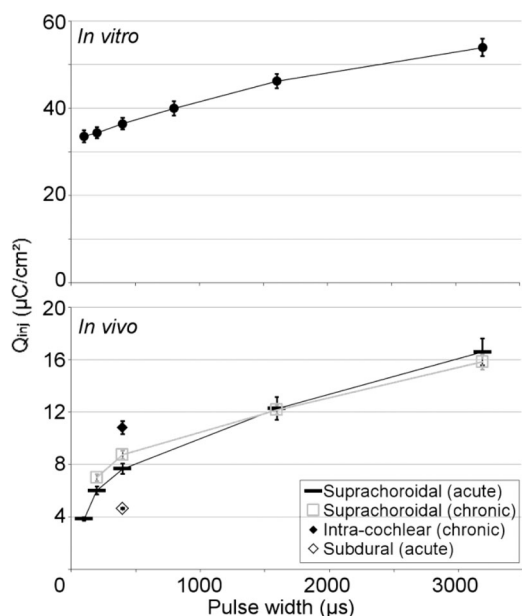


Fig. 4. Plot of the Q_{inj} of Pt electrodes for various pulse widths *in vitro* (black circles, $n = 7$), in acutely (black bars, $n = 18$) and chronically (gray squares, $n = 10$) implanted electrodes in the suprachoroidal space, in chronically implanted intracochlear electrodes (closed diamond, $n = 3$), and in acutely implanted subdural electrodes (open diamond, $n = 4$). Error bars indicate standard error.

to 8.7 times greater than *in vivo*. As expected, *in vitro* Q_{inj} was lower compared to studies using smaller electrodes [37], [40].

Compared to this study, Rose and Robblee reported higher Q_{inj} *in vitro* with pulse widths of 200 μs even though the electrodes were larger than those used in this study [23]. Rose and Robblee stimulated electrodes at a rate of 50 pulses/s, which is far greater than the 4 pulses/s used in the present study. Irreversible electrochemical reactions during the cathodic phase can cause the interpulse potential to become more positive. Although the interpulse potential will eventually return to the open-circuit potential, successive pulses may cause a “ratcheting” effect, leading to a more positive interpulse potential [19]. Higher pulse rates allow less time for the interpulse potential to return to a level that is closer to the open-circuit potential and this enhances the “ratcheting” effect and, thus, the value of E_{mc} will be less negative. This may lead to an overestimation of Q_{inj} . In this study, stimulation rates were selected to ensure that E_{mc} measurements were not significantly affected by drifts in interpulse potential.

Q_{inj} increased with pulse width and this has been shown previously for iridium oxide [26], as well as Pt [62] electrodes. We have shown that this dependence of Q_{inj} on pulse width continues at pulse widths $>400 \mu s$. Longer pulse widths allow more time for reactions such as hydrogen atom plating/stripping and Pt oxidation/reduction to occur which results in an increased Q_{inj} compared to shorter pulse durations [23]. The contribution of oxygen reduction to the Q_{inj} is also greater at longer pulse widths [35]. The dependence of Q_{inj} on pulse width was not observed by Brummer and Turner [36]. This is likely to be due to differences in the way water electrolysis was identified. Although Q_{inj} can be increased by lengthening the pulse width,

caution is advised since the rate of Pt dissolution also increases with pulse width [67]. However, Pt dissolution is inhibited by protein [68] and decreases with time *in vivo* [69]. Also, no studies have investigated the chronic tissue response and electrode stability following stimulation using long pulse widths with Pt electrodes. Furthermore, the effect of pulse width on Q_{inj} may vary with electrode geometry and the stimulation parameters.

The water window *in vivo* was found to be similar to that found *in vitro* and was consistent with the established literature [70], [71]. The suprachoroidal Q_{inj} was only 11.5% to 30.8% of Q_{inj} *in vitro*. The Q_{inj} of the cortical surface was approximately 12.7% of the Q_{inj} *in vitro* with a 400- μs pulse width, which is a similar reduction of Q_{inj} in activated iridium oxide electrodes implanted in the cortex [32]. A reduction in Q_{inj} *in vivo* can be expected due to differences between PBS and the physiological environment, including the presence of organic species and differences in the electrolyte concentration [21]. The reduction in the *in vivo* Q_{inj} was greater at short pulse widths compared to long pulse widths. The diffusion of counter ions *in vivo* may be restricted by the presence of tissues [27]. This could reduce Q_{inj} *in vivo*, particularly at short pulse widths when higher current densities are used.

The similarities in the chronic and acute suprachoroidal Q_{inj} concurs with previous reports that chronic implantation does not damage Pt electrodes [72]. Furthermore, the results suggest that differences in the acute and chronic tissue response did not have a major impact on Q_{inj} . A significant amount of fibrosis is unlikely to have occurred during the acute stimulation period of 1 to 72 h although a chronically implanted electrode array is expected to be encapsulated in fibrotic tissue. However, recent work has shown that the fibrosis around electrode arrays of the same design, implanted for three months, was minimal [73]. Since the electrodes used in this study were recessed, the tissues adjacent to the electrodes may not have been in contact with the entire surface of the electrodes, particularly in the acute setting. However, as there was minimal difference between chronic and acute Q_{inj} , the recess is likely to have had a minimal effect on Q_{inj} . There were minor variations in the acute and chronic tissue resistances as illustrated by the difference in the access voltage of the acute and chronic voltage transient [see Fig. 3]. Slight intersubject variations are inherent in *in vivo* studies, which may account for the differences in tissue resistance. However, the access voltage is not included in the calculation of E_{mc} and, thus, does not contribute to Q_{inj} [21].

The access voltage is typically calculated from the voltage step of the voltage excursion waveform at the beginning or end of cathodic or anodic phases. However, the voltage step of the waveform at the beginning of the cathodic phase is larger than at the end, as demonstrated in [see Fig. 3]. This was likely a result of parasitic capacitance in the outputs of the stimulator, which is typical of constant-current stimulators. In between stimulation pulses, the parasitic capacitance in the stimulator is charged up to supply voltage. At the stimulus onset, the entire supply voltage is applied to the active electrode, which results in a voltage step which is greater than the access voltage alone [74]. E_{mc} was measured during the interphase gap and, thus, calculation of the access voltage was not required to determine Q_{inj} .

The cathodic and anodic phases of the voltage waveforms are slightly asymmetric [see Fig. 3]. The series capacitor accumulates charge during the cathodic phase and discharges during the anodic phase. If the potential delivered by the capacitor during the anodic phase is greater than the sum of that required to overcome the access resistance and deliver the desired current, the anodic and cathodic phases will be asymmetric. This is especially evident at the beginning of the anodic phase, where there is a voltage step that is greater than the expected access voltage. At the anodic phase offset, the working and counter electrodes are shorted allowing the capacitor to discharge and causing the potential to return to the interpulse potential with a larger step than would be expected from the access voltage alone. The anodic phase waveform is not used to calculate E_{mc} and, thus, Q_{inj} was not affected by the asymmetry.

The Q_{inj} in the suprachoroidal space was not different to the Q_{inj} using intracochlear electrodes, but was greater than that found on the cortical surface and this is likely due to differences in the anatomy and physiology of each location. The intracochlear electrode is implanted into the scala tympani, which is a fluid filled cavity where there may be less obstruction of diffusing electrolytes and the degree of fibrosis is highly variable. Suprachoroidal electrodes face the choroid which is well perfused and ensures a ready supply of electrolytes, although the blood vessel walls may hinder its availability to the electrode surface. This highlights the importance of understanding the effect of the implant location on Q_{inj} and the need for *in vivo* testing in a location which is similar to the intended application.

Q_{inj} can be measured with methods other than voltage transients [33], [36] and this may produce different outcomes. For example, the method for measuring Q_{inj} used by Brummer and Turner [36], [41] examined the voltage excursion waveform shape. An asymptote in the waveform during the cathodic or anodic phase was used to indicate the evolution of hydrogen or oxygen, respectively. This asymptotic behaviour is not evident at the end of the cathodic phase *in vivo* and the slope remains steep [see Fig. 3]. Thus, Q_{inj} *in vivo* determined using the method by Brummer and Turner may be higher than that found in the present study. However, since the animals used in this study were also part of separate studies where retinal and cochlear pathology were important outcomes, determination of Q_{inj} with this method was not investigated.

Although we found that Q_{inj} was very small *in vivo*, histopathological examination of cochleae which were chronically stimulated with charge densities of up to $52 \mu\text{C}/\text{cm}^2$ with pulsewidths up to $200 \mu\text{s}$ showed no correlation between charge density and damage to surrounding structures [75]–[78]. Similarly, acute cortical stimulation with a charge density of $40 \mu\text{C}/\text{cm}^2$ and a pulsewidth of $100 \mu\text{s}$ resulted in only mild neural damage [9]. These charge densities are far greater than those defined as Q_{inj} *in vivo* in this study. Therefore, although Q_{inj} is sometimes used to define safe *in vivo* stimulation limits [79], [80], the clinical relevance of this measure, at least determined using voltage transients, is questionable.

The polarization of electrodes beyond the water window causes water electrolysis but tissue damage may not ensue. The evolution of oxygen and hydrogen gas can physically damage

tissues if gas bubbles are formed. However, if the rate of gas production is not excessive, physical gassing may not occur since the gasses can dissolve into the tissue [81], [82]. Electrolysis of water produces OH^- and H^+ , and this may result in pH changes. However, physiological pH buffers may minimize pH shifts and, if both water oxidation and reduction occur, some H^+ ions may be neutralized by OH^- ions [81]. By using charge balanced stimulation with capacitive coupling and electrode shorting, net pH changes can be minimized [22]. It should be noted that the pH close to the electrodes may change during the stimulation pulse and this may cause tissue damage [66].

In the present study, we have adapted the predominantly *in vitro* technique of using potential transients to measure Q_{inj} to the *in vivo* situation. Factors such as the permittivity of the tissue and positioning of the reference electrode may affect the measured Q_{inj} *in vivo*. Thus, the measured Q_{inj} *in vivo* may be less accurate compared with *in vitro* measurements. Further investigation into the accuracy of measuring Q_{inj} *in vivo* may be necessary. Nonetheless, this method of determining Q_{inj} is standard practice for evaluating biomedical electrodes *in vivo* [32], [60]. An alternative to measuring Q_{inj} would be to perform CV or electrochemical impedance spectroscopy. In order to determine practical guidelines on safe *in vivo* stimulation limits, chronic stimulation in a suitable animal model will be the most informative approach.

Measuring Q_{inj} *in vitro* in a three-electrode model is a useful tool for comparing different materials, geometries, or stimulation protocols. However, the composition of the electrolyte [30] and differences in experimental setup can have significant effects on the findings. Thus, when comparing Q_{inj} *in vitro*, the experimental setup should be comparable. It may also be advantageous to use capacitive coupling [22] and shorting between electrodes [59] to minimize residual direct current which could otherwise lead to variations in Q_{inj} depending on the equipment and protocols used. It is also important to remember that findings using *in vitro* models may differ *in vivo* [21].

In summary, the *in vitro* Q_{inj} of Pt macroelectrodes varied from 34 to $54 \mu\text{C}/\text{cm}^2$ for pulsewidths of 100 to $3200 \mu\text{s}$, increasing with pulsewidth. Q_{inj} was reduced to 11.5% to 30.8% of the *in vitro* levels when electrodes were placed in the suprachoroidal space acutely or chronically. There were significant differences in Q_{inj} when electrodes were placed on the cortical surface but not the cochlea. The *in vivo* Q_{inj} determined using voltage transients was found to significantly underestimate the safe stimulation limits determined using histopathological analysis found in the literature, possibly, because tissues can tolerate a degree of water electrolysis. This suggests that an alternative method for determining safe stimulation limits *in vivo* is required. Ultimately, chronic stimulation and histological examination using the electrode array and stimulation site for which the device is intended for is always required for the most rigorous measure of safe charge injection limits.

ACKNOWLEDGMENT

The Bionics Institute would like to thank the Victorian Government through its Operational Infrastructure Support Program

and the Bertalli Family Trust. Also, the authors would like to thank Dr. D. Garrett, Dr. S. John, Dr. J. Fallon, Dr. S. Irving, and Dr. S. Mergen for technical support; A/Prof. C. Williams, Prof. P. Selligman, Dr. D. McCreery, and Prof. S. Cogan for valuable discussions; H. Feng and Dr. J. Villalobos for electrode fabrication; Dr. P. Allen for surgical procedures; A. Saunders, and M. McPhedran for animal care; Dr. R. Cicione, F. Aplin, and Dr. P. Atkinson for data collection; Dr. S. Pierce for veterinary support and; staff at the Biological Research Centre, Royal Victorian Eye, and Ear Hospital, Melbourne for animal support.

REFERENCES

- [1] R. Shepherd, K. Verhoeven, J. Xu, F. Risi, J. Fallon, and A. Wise, "An improved cochlear implant electrode array for use in experimental studies," *Hear. Res.*, vol. 277, nos. 1/2, pp. 20–27, Jul. 2011.
- [2] M. Cosetti and J. T. Roland Jr., "Cochlear implant electrode insertion," *Operative Techn. Otolaryngol.-Head Neck Surg.*, vol. 21, no. 4, pp. 223–232, 2010.
- [3] D. Yanai, J. D. Weiland, M. Mahadevappa, R. J. Greenberg, I. Fine, and M. S. Humayun, "Visual performance using a retinal prosthesis in three subjects with retinitis pigmentosa," *Amer. J. Ophthalmol.*, vol. 143, no. 5, pp. 820–827, May 2007.
- [4] M. N. Shivdasani, C. D. Luu, R. Cicione, J. B. Fallon, P. J. Allen, J. Leuenberger, G. J. Suaning, N. H. Lovell, R. K. Shepherd, and C. E. Williams, "Evaluation of stimulus parameters and electrode geometry for an effective suprachoroidal retinal prosthesis," *J. Neural Eng.*, vol. 7, no. 3, pp. 1–11, Jun. 2010.
- [5] T. Fujikado, M. Kamei, H. Sakaguchi, H. Kanda, T. Morimoto, Y. Ikuno, K. Nishida, H. Kishima, T. Maruo, K. Konoma, and M. Ozawa, "Testing of semichronically implanted retinal prosthesis by suprachoroidal-transretinal stimulation in patients with retinitis pigmentosa," *Invest Ophthalmol. Vis. Sci.*, vol. 52, no. 7, pp. 4726–4733, Jun. 2011.
- [6] G. S. Brindley and W. S. Lewin, "The sensations produced by electrical stimulation of the visual cortex," *J. Physiol.*, vol. 196, no. 2, pp. 479–493, May 1968.
- [7] W. H. Dobbelle and M. G. Mladejovsky, "Phosphenes produced by electrical stimulation of human occipital cortex, and their application to the development of a prosthesis for the blind," *J. Physiol.*, vol. 243, no. 2, pp. 553–576, Dec. 1974.
- [8] E. J. Plautz, S. Barbay, S. B. Frost, K. M. Friel, N. Dancause, E. V. Zoubina, A. M. Stowe, B. M. Quaney, and R. J. Nudo, "Post-infarct cortical plasticity and behavioral recovery using concurrent cortical stimulation and rehabilitative training: A feasibility study in primates," *Neurol. Res.*, vol. 25, no. 8, pp. 801–810, Dec. 2003.
- [9] T. G. Yuen, W. F. Agnew, L. A. Bullara, S. Jacques, and D. B. McCreery, "Histological evaluation of neural damage from electrical stimulation: Considerations for the selection of parameters for clinical application," *Neurosurgery*, vol. 9, no. 3, pp. 292–299, Sep. 1981.
- [10] D. B. McCreery, W. F. Agnew, T. G. Yuen, and L. Bullara, "Charge density and charge per phase as cofactors in neural injury induced by electrical stimulation," *IEEE Trans. Biomed. Eng.*, vol. 37, no. 10, pp. 996–1001, Oct. 1990.
- [11] W. F. Agnew, T. G. Yuen, and D. B. McCreery, "Morphologic changes after prolonged electrical stimulation of the cat's cortex at defined charge densities," *Exp. Neurol.*, vol. 79, no. 2, pp. 397–411, Feb. 1983.
- [12] R. V. Shannon, J. K. Moore, D. B. McCreery, and F. Portillo, "Threshold-distance measures from electrical stimulation of human brainstem," *IEEE Trans. Rehabil. Eng.*, vol. 5, no. 1, pp. 70–74, Mar. 1997.
- [13] R. V. Shannon and S. R. Otto, "Psychophysical measures from electrical stimulation of the human cochlear nucleus," *Hear. Res.*, vol. 47, nos. 1/2, pp. 159–168, Aug. 1, 1990.
- [14] K. Wang, X. Q. Li, X. X. Li, W. H. Pei, H. D. Chen, and J. Q. Dong, "Efficacy and reliability of long-term implantation of multi-channel microelectrode arrays in the optical nerve sheath of rabbit eyes," *Vis. Res.*, vol. 51, no. 17, pp. 1897–906, Sep. 1, 2011.
- [15] K. H. Polasek, H. A. Hoyer, M. W. Keith, and D. J. Tyler, "Human nerve stimulation thresholds and selectivity using a multi-contact nerve cuff electrode," *IEEE Trans. Neural Syst. Rehabil. Eng.*, vol. 15, no. 1, pp. 76–82, Mar. 2007.
- [16] J. Delbeke, M. C. Wanet-Defalque, B. Gerard, M. Troosters, G. Michaux, and C. Veraart, "The microsystems based visual prosthesis for optic nerve stimulation," *Artif. Organs.*, vol. 26, no. 3, pp. 232–234, Mar. 2002.
- [17] V. Chowdhury, J. W. Morley, and M. T. Coroneo, "Development of an extraocular retinal prosthesis: Evaluation of stimulation parameters in the cat," *J. Clin. Neurosci.*, vol. 15, no. 8, pp. 900–906, Aug. 2008.
- [18] M. D. Tarler and J. T. Mortimer, "Selective and independent activation of four motor fascicles using a four contact nerve-cuff electrode," *IEEE Trans. Neural Syst. Rehabil. Eng.*, vol. 12, no. 2, pp. 251–257, Jun. 2004.
- [19] D. R. Merrill, M. Bikson, and J. G. Jefferys, "Electrical stimulation of excitable tissue: Design of efficacious and safe protocols," *J. Neurosci. Methods*, vol. 141, no. 2, pp. 171–198, Feb. 15, 2005.
- [20] S. B. Brummer and M. J. Turner, "Electrochemical considerations for safe electrical stimulation of the nervous system with platinum electrodes," *IEEE Trans. Biomed. Eng.*, vol. 24, no. 1, pp. 59–63, Jan. 1977.
- [21] S. F. Cogan, "Neural stimulation and recording electrodes," *Annu. Rev. Biomed. Eng.*, vol. 10, pp. 275–309, 2008.
- [22] C. Q. Huang, P. M. Carter, and R. K. Shepherd, "Stimulus induced pH changes in cochlear implants: An in vitro and in vivo study," *Ann. Biomed. Eng.*, vol. 29, no. 9, pp. 791–802, Sep. 2001.
- [23] T. L. Rose and L. S. Robblee, "Electrical stimulation with Pt electrodes. VIII. Electrochemically safe charge injection limits with 0.2 ms pulses," *IEEE Trans. Biomed. Eng.*, vol. 37, no. 11, pp. 1118–1120, Nov. 1990.
- [24] E. M. Hudak, J. T. Mortimer, and H. B. Martin, "Platinum for neural stimulation: Voltammetry considerations," *J. Neural Eng.*, vol. 7, no. 2, pp. 1–7, Apr. 2010.
- [25] B. Rosenberg, L. Vancamp, and T. Krigas, "Inhibition of cell division in *Escherichia coli* by electrolysis products from a platinum electrode," *Nature*, vol. 205, pp. 698–699, Feb. 13, 1965.
- [26] S. Negi, R. Bhandari, L. Rieth, and F. Solzbacher, "In vitro comparison of sputtered iridium oxide and platinum-coated neural implantable microelectrode arrays," *Biomed. Mater.*, vol. 5, no. 1, p. 15007, Feb. 2010.
- [27] S. F. Cogan, "In vivo and in vitro differences in the charge-injection and electrochemical properties of iridium oxide electrodes," in *Proc. IEEE Conf. Eng. Med. Biol. Soc.*, 2006, vol. 1, pp. 882–885.
- [28] M. F. Suesserman, F. A. Spelman, and J. T. Rubinstein, "In vitro measurement and characterization of current density profiles produced by non-recessed, simple recessed, and radially varying recessed stimulating electrodes," *IEEE Trans. Biomed. Eng.*, vol. 38, no. 5, pp. 401–408, May 1991.
- [29] M. R. Behrend, A. K. Ahuja, and J. D. Weiland, "Dynamic current density of the disk electrode double-layer," *IEEE Trans. Biomed. Eng.*, vol. 55, no. 3, pp. 1056–1062, Mar. 2008.
- [30] S. F. Cogan, P. R. Troyk, J. Ehrlich, C. M. Gasbarro, and T. D. Plante, "The influence of electrolyte composition on the in vitro charge-injection limits of activated iridium oxide (AIROF) stimulation electrodes," *J. Neural Eng.*, vol. 4, no. 2, pp. 79–86, Jun. 2007.
- [31] S. R. Kane, S. F. Cogan, J. Ehrlich, T. D. Plante, D. B. McCreery, and P. R. Troyk, "Electrical performance of penetrating microelectrodes chronically implanted in cat cortex," *IEEE Trans. Biomed. Eng.*, vol. 60, no. 8, pp. 2153–2160, Feb. 26, 2013.
- [32] Z. Hu, P. R. Troyk, T. P. Brawn, D. Margoliash, and S. F. Cogan, "In vitro and in vivo charge capacity of AIROF microelectrodes," in *Proc. IEEE Conf. Eng. Med. Biol. Soc.*, 2006, vol. 1, pp. 886–889.
- [33] S. Musa, D. R. Rand, C. Batic, W. Eberle, B. Nuttin, and G. Borghs, "Coulometric detection of irreversible electrochemical reactions occurring at Pt microelectrodes used for neural stimulation," *Anal. Chem.*, vol. 83, no. 11, pp. 4012–4022, Jun. 1, 2011.
- [34] R. K. R. Phillips, S. Omanovic, and S. G. Roscoe, "A cyclic voltammetry study of the adsorption of alcohol dehydrogenase (HLADH) onto a platinum electrode," *Electrochem. Commun.*, vol. 2, no. 11, pp. 805–809, 2000.
- [35] S. F. Cogan, J. Ehrlich, T. D. Plante, M. D. Gingerich, and D. B. Shire, "Contribution of oxygen reduction to charge injection on platinum and sputtered iridium oxide neural stimulation electrodes," *IEEE Trans. Biomed. Eng.*, vol. 57, no. 9, pp. 2313–2321, Sep. 2010.
- [36] S. B. Brummer and M. J. Turner, "Electrical stimulation with Pt electrodes: II—Estimation of maximum surface redox (theoretical non-gassing) limits," *IEEE Trans. Biomed. Eng.*, vol. 24, no. 5, pp. 440–443, Sep. 1977.
- [37] R. A. Green, P. B. Matteucci, R. T. Hassarati, B. Giraud, C. W. Dodds, S. Chen, P. J. Byrnes-Preston, G. J. Suaning, L. A. Poole-Warren, and N. H. Lovell, "Performance of conducting polymer electrodes for stimulating neuroprosthetics," *J. Neural Eng.*, vol. 10, no. 1, pp. 1–11, Feb. 2013.
- [38] T. Boretius, J. Badia, A. Pascual-Font, M. Schuettler, X. Navarro, K. Yoshida, and T. Stieglitz, "A transverse intrafascicular multichannel

- electrode (TIME) to interface with the peripheral nerve," *Biosens. Bioelectron.*, vol. 26, no. 1, pp. 62–69, Sep. 15, 2010.
- [39] M. Schuettler, "Electrochemical properties of platinum electrodes in vitro: Comparison of six different surface qualities," in *Proc. IEEE Conf. Eng. Med. Biol. Soc.*, 2007, vol. 2007, pp. 186–189.
- [40] R. A. Green, R. T. Hassarati, L. Bouchinet, C. S. Lee, G. L. Cheong, J. F. Yu, C. W. Dodds, G. J. Suaning, L. A. Poole-Warren, and N. H. Lovell, "Substrate dependent stability of conducting polymer coatings on medical electrodes," *Biomaterials*, vol. 33, no. 25, pp. 5875–5886, Sep. 2012.
- [41] S. B. Brummer and M. J. Turner, "Electrical stimulation with Pt electrodes: I—A method for determination of "real" electrode areas," *IEEE Trans. Biomed. Eng.*, vol. 24, no. 5, pp. 436–439, Sep. 1977.
- [42] R. K. Shepherd, M. N. Shivdasani, D. A. Nayagam, C. E. Williams, and P. J. Blamey, "Visual prostheses for the blind," *Trends Biotechnol.*, vol. 31, no. 10, pp. 562–571, Oct. 2013.
- [43] Y. T. Wong, S. C. Chen, J. M. Seo, J. W. Morley, N. H. Lovell, and G. J. Suaning, "Focal activation of the feline retina via a suprachoroidal electrode array," *Vis. Res.*, vol. 49, no. 8, pp. 825–833, Mar. 2009.
- [44] J. S. Shyu, M. Maia, J. D. Weiland, T. Ohearn, S. J. Chen, E. Margalit, S. Suzuki, and M. S. Humayun, "Electrical stimulation in isolated rabbit retina," *IEEE Trans. Neural Syst. Rehabil. Eng.*, vol. 14, no. 3, pp. 290–298, Sep. 2006.
- [45] J. F. Rizzo III, J. Wyatt, J. Loewenstein, S. Kelly, and D. Shire, "Methods and perceptual thresholds for short-term electrical stimulation of human retina with microelectrode arrays," *Invest Ophthalmol. Vis. Sci.*, vol. 44, no. 12, pp. 5355–5361, Dec. 2003.
- [46] A. Horsager, S. H. Greenwald, J. D. Weiland, M. S. Humayun, R. J. Greenberg, M. J. McMahon, G. M. Boynton, and I. Fine, "Predicting visual sensitivity in retinal prosthesis patients," *Invest Ophthalmol. Vis. Sci.*, vol. 50, no. 4, pp. 1483–1491, Apr. 2009.
- [47] K. Nakauchi, T. Fujikado, H. Kanda, S. Kusaka, M. Ozawa, H. Sakaguchi, Y. Ikuno, M. Kamei, and Y. Tano, "Threshold suprachoroidal-transretinal stimulation current resulting in retinal damage in rabbits," *J. Neural Eng.*, vol. 4, no. 1, pp. S50–S57, Mar. 2007.
- [48] C. A. Miller, P. J. Abbas, B. K. Robinson, J. T. Rubinstein, and A. J. Matsuoka, "Electrically evoked single-fiber action potentials from cat: Responses to monopolar, monophasic stimulation," *Hear. Res.*, vol. 130, nos. 1/2, pp. 197–218, Apr. 1999.
- [49] C. A. Miller, P. J. Abbas, and C. J. Brown, "Electrically evoked auditory brainstem response to stimulation of different sites in the cochlea," *Hear. Res.*, vol. 66, no. 2, pp. 130–142, Apr. 1993.
- [50] A. J. Matsuoka, P. J. Abbas, J. T. Rubinstein, and C. A. Miller, "The neuronal response to electrical constant-amplitude pulse train stimulation: additive Gaussian noise," *Hear. Res.*, vol. 149, nos. 1/2, pp. 129–137, Nov. 2000.
- [51] I. Hochmair-Desoyer and E. S. Hochmair, "An eight channel scala tympani electrode for auditory prostheses," *IEEE Trans. Biomed. Eng.*, vol. 27, no. 1, pp. 44–50, Jan. 1980.
- [52] H. Kasi, W. Hasenkamp, G. Cosendai, A. Bertsch, and P. Renaud, "Simulation of epiretinal prostheses—evaluation of geometrical factors affecting stimulation thresholds," *J. Neuroeng. Rehabil.*, vol. 8, pp. 1–10, 2011.
- [53] A. Ray, E. J. Lee, M. S. Humayun, and J. D. Weiland, "Continuous electrical stimulation decreases retinal excitability but does not alter retinal morphology," *J. Neural Eng.*, vol. 8, no. 4, pp. 1–11, Aug. 2011.
- [54] C. A. Miller, J. Woo, P. J. Abbas, N. Hu, and B. K. Robinson, "Neural masking by sub-threshold electric stimuli: Animal and computer model results," *J. Assoc. Res. Otolaryngol.*, vol. 12, no. 2, pp. 219–232, Apr. 2011.
- [55] J. Villalobos, P. J. Allen, M. F. McCombe, M. Ulaganathan, E. Zamir, D. C. Ng, R. K. Shepherd, and C. E. Williams, "Development of a surgical approach for a wide-view suprachoroidal retinal prosthesis: Evaluation of implantation trauma," *Graefes Arch. Clin. Exp. Ophthalmol.*, vol. 250, no. 3, pp. 399–407, Mar. 2012.
- [56] P. J. Blamey, N. C. Sinclair, K. Slater, H. J. McDermott, T. Perera, P. N. Dimitrov, M. Varsamidis, L. N. Ayton, R. H. Guymer, and C. D. Luu, "Psychophysics of a suprachoroidal retinal prosthesis," presented at the *Assoc. Res. Vis. Ophthalmol. Annu. Meet.*, Seattle, Washington, USA, 2013.
- [57] J. B. Fallon, D. R. Irvine, and R. K. Shepherd, "Cochlear implant use following neonatal deafness influences the cochleotopic organization of the primary auditory cortex in cats," *J. Comp. Neurol.*, vol. 512, no. 1, pp. 101–114, Jan. 1, 2009.
- [58] J. Wang, "Study of electrode reactions and interfacial properties," in *Analytical electrochemistry*, 3rd ed. Hoboken, NJ, USA: Wiley, 2006, pp. 29–37.
- [59] C. Q. Huang, R. K. Shepherd, P. M. Carter, P. M. Seligman, and B. Tabor, "Electrical stimulation of the auditory nerve: Direct current measurement in vivo," *IEEE Trans. Biomed. Eng.*, vol. 46, no. 4, pp. 461–470, Apr. 1999.
- [60] S. R. Kane, S. F. Cogan, J. Ehrlich, T. D. Plante, D. B. McCreery, and P. R. Troyk, "Electrical performance of penetrating microelectrodes chronically implanted in cat cortex," *IEEE Trans. Biomed. Eng.*, vol. 60, no. 8, pp. 2153–2160, Aug. 2013.
- [61] A. E. Hadjinicolaou, R. T. Leung, D. J. Garrett, K. Ganesan, K. Fox, D. A. Nayagam, M. N. Shivdasani, H. Meffin, M. R. Ibbotson, S. Prawer, and B. J. O'Brien, "Electrical stimulation of retinal ganglion cells with diamond and the development of an all diamond retinal prosthesis," *Biomaterials*, vol. 33, no. 24, pp. 5812–5820, Aug. 2012.
- [62] S. F. Cogan, P. R. Troyk, J. Ehrlich, and T. D. Plante, "In vitro comparison of the charge-injection limits of activated iridium oxide (AIROF) and platinum-iridium microelectrodes," *IEEE Trans. Biomed. Eng.*, vol. 52, no. 9, pp. 1612–1614, Sep. 2005.
- [63] J. D. Weiland, D. J. Anderson, and M. S. Humayun, "In vitro electrical properties for iridium oxide versus titanium nitride stimulating electrodes," *IEEE Trans. Biomed. Eng.*, vol. 49, no. 12, pp. 1574–1579, Dec. 2002.
- [64] S. F. Cogan, T. D. Plante, and J. Ehrlich, "Sputtered-iridium oxide films (SIROFs) for low-impedance neural stimulation and recording electrodes," in *Proc. IEEE Conf. Eng. Med. Biol. Soc.*, 2004, vol. 6, pp. 4153–4156.
- [65] S. F. Cogan, P. R. Troyk, J. Ehrlich, T. D. Plante, and D. E. Detlefsen, "Potential-biased, asymmetric waveforms for charge-injection with activated iridium oxide (AIROF) neural stimulation electrodes," *IEEE Trans. Biomed. Eng.*, vol. 53, no. 2, pp. 327–332, Feb. 2006.
- [66] H. Tashiro, Y. Terasawa, K. Osawa, M. Ozawa, T. Noda, J. Ohta, and T. Fujikado, "In vivo characterisation of electrochemically-treated platinum bulk electrodes for retinal prostheses," presented at the *Assoc. Res. Vis. Ophthalmol. Annu. Meet.*, Fort Lauderdale, FL, USA, 2012.
- [67] J. McHardy, L. S. Robblee, J. M. Marston, and S. B. Brummer, "Electrical stimulation with Pt electrodes. IV. Factors influencing Pt dissolution in inorganic saline," *Biomaterials*, vol. 1, no. 3, pp. 129–134, Jul. 1980.
- [68] L. S. Robblee, J. McHardy, J. M. Marston, and S. B. Brummer, "Electrical stimulation with Pt electrodes. V. The effect of protein on Pt dissolution," *Biomaterials*, vol. 1, no. 3, pp. 135–139, Jul. 1980.
- [69] L. S. Robblee, J. McHardy, W. F. Agnew, and L. A. Bullara, "Electrical stimulation with Pt electrodes. VII. Dissolution of Pt electrodes during electrical stimulation of the cat cerebral cortex," *J. Neurosci. Methods*, vol. 9, no. 4, pp. 301–308, Dec. 1983.
- [70] Y. Terasawa, H. Tashiro, Y. Nakano, K. Osawa, M. Ozawa, "Safety assessment of semichronic suprachoroidal electrical stimulation to rabbit retina," in *Proc. IEEE Conf. Eng. Med. Biol. Soc.*, Jul. 2013, vol. 2013, pp. 3567–3570.
- [71] L. Colodetti, J. D. Weiland, S. Colodetti, A. Ray, M. J. Seiler, D. R. Hinton, M. S. Humayun, "Pathology of damaging electrical stimulation in the retina," *Exp. Eye Res.*, vol. 85, no. 1, pp. 23–33, Jul. 2007.
- [72] R. K. Shepherd, M. T. Murray, M. E. Houghton, and G. M. Clark, "Scanning electron microscopy of chronically stimulated platinum intracochlear electrodes," *Biomaterials*, vol. 6, no. 4, pp. 237–242, Jul. 1985.
- [73] J. Villalobos, D. A. Nayagam, P. J. Allen, Allen, P. McKelvie, C. D. Luu, L. N. Ayton, A. L. Freemantle, M. McPhedran, M. Basa, C. C. McGowan, R. K. Shepherd, and C. E. Williams, "A wide-field suprachoroidal retinal prosthesis is stable and well tolerated following chronic implantation," *Invest Ophthalmol. Vis. Sci.*, vol. 54, pp. 3751–3762, Apr. 23, 2013.
- [74] P. M. Seligman, M. N. Shivdasani, S. E. John, and D. A. Nayagam, "Electrode models and practical stimulator behaviour," presented at the *2nd Int. Conf. Med. Bionics—Neural Interfaces Damaged Nerves*, Phillip Island, VIC, Australia, 2011.
- [75] D. Ni, R. K. Shepherd, H. L. Seldon, S. A. Xu, G. M. Clark, and R. E. Millard, "Cochlear pathology following chronic electrical stimulation of the auditory nerve. I: Normal hearing kittens," *Hear. Res.*, vol. 62, no. 1, pp. 63–81, Sep. 1992.
- [76] R. K. Shepherd, G. M. Clark, and R. C. Black, "Chronic electrical stimulation of the auditory nerve in cats. Physiological and histopathological results," *Acta Otolaryngol. Suppl.*, vol. 399, pp. 19–31, 1983.
- [77] R. K. Shepherd, J. Matsushima, R. L. Martin, and G. M. Clark, "Cochlear pathology following chronic electrical stimulation of the auditory nerve: II. Deafened kittens," *Hear. Res.*, vol. 81, nos. 1/2, pp. 150–166, Dec. 1994.
- [78] J. Xu, R. K. Shepherd, R. E. Millard, and G. M. Clark, "Chronic electrical stimulation of the auditory nerve at high stimulus rates: A physiological and histopathological study," *Hear. Res.*, vol. 105, nos. 1/2, pp. 1–29, Mar. 1997.

- [79] J. Ohta, T. Tokuda, K. Kagawa, T. Furumiyu, A. Uehara, Y. Terasawa, M. Ozawa, T. Fujikado, Y. Tano, "Silicon LSI-based smart stimulators for retinal prosthesis," *IEEE Eng. Med. Biol. Mag.*, vol. 25, no. 5, pp. 47–59, Sep./Oct., 2006.
- [80] T. Nyberg, A. Shimada, and K. Torimitsu, "Ion conducting polymer microelectrodes for interfacing with neural networks," *J. Neurosci. Methods*, vol. 160, no. 1, pp. 16–25, Feb. 15, 2007.
- [81] J. T. Mortimer, D. Kaufman, and U. Roessman, "Intramuscular electrical stimulation: Tissue damage," *Ann. Biomed. Eng.*, vol. 8, no. 3, pp. 235–244, 1980.
- [82] S. B. Brummer, L. S. Robblee, and F. T. Hambrecht, "Criteria for selecting electrodes for electrical stimulation: theoretical and practical considerations," *Ann. N Y Acad. Sci.*, vol. 405, pp. 159–171, 1983.



Ronald T. Leung received the B.Eng.(Hons) degree in biomedical engineering from The University of Melbourne, Parkville, Vic., Australia in 2010, where he is currently working toward the Ph.D. degree in retinal prosthesis safety studies at the Bionics Institute and Department of Pathology.

In 2008, he joined the Bionics Institute for one year as a Research Student. His research interests include implantable devices, particularly in electrochemistry, electrophysiology, and pathology.

Mr. Leung is a Member of the Australian Society for Medical Research and the Australian Neuroscience Society. He received the Harold Mitchell Foundation Travel Scholarship.



Mohit N. Shivdasani migrated from India to Australia in 2003 to pursue a Master's degree in Biomedical Engineering at La Trobe University. He then went on to complete a Ph.D. degree in 2009 at the Bionics Institute, Melbourne on Auditory Brainstem Implants, devices that electrically stimulate the auditory brainstem to restore hearing to deaf people who cannot benefit from a cochlear implant.

He is now part of a large multidisciplinary team that developed a retinal prosthesis through Bionic Vision Australia and played a major role in the pre-clinical testing of devices prior to clinical trials. Since the award of his PhD, Dr Shivdasani has published 27 research papers including six as first author in prestigious international scientific journals and has won seven awards including the 2006 Young Biomedical Engineer Award presented by Engineers Australia.

He is also so far the only double recipient of the Harold Mitchell Travelling Fellowship, both as a postgraduate student and as a postdoctoral researcher. He is currently a member of the Australian Neuroscience Society and the Association for Research in Vision and Ophthalmology.



David A. X. Nayagam (M'07) was born in Sri Lanka in 1978. He received the B.Sc. and B.E.(Hons.) degrees in neuroscience and electrical engineering from The University of Melbourne, Parkville, Vic., Australia, in 2001. After a one year hiatus backpacking around the globe, he received the Ph.D. degree in auditory neuroscience (electrophysiology) from The University of Melbourne in 2007.

He is currently a Research Fellow at the Bionics Institute of Australia (formerly the Bionic Ear Institute), Melbourne, where he conducts multidisciplinary research into the safe and efficacious use of nanotechnology and bionic devices. He is presently a Member of the team which successfully developed and implanted a retinal prosthesis ("Bionic Eye") into blind patients, in a world-first clinical trial of its kind. He also holds an honorary position in the University of Melbourne's Department of Pathology. In 2009, he was one of 22 candidates, from 8 413 suitably qualified applicants, to reach the final stage of selection in the European Space Agency's astronaut recruitment program.

Dr. Nayagam has been a Foundational Member of the Australian government's Space Industry Innovation Council since 2009 where he has contributed to the creation of Australia's inaugural space policy (released: April 2013). He is a Member of the Australian Neuroscience Society, the Royal Australian and New Zealand College of Ophthalmologists, and the Association for Research in Vision and Ophthalmology.



Robert K. Shepherd (M'09) was born in Portland, Vic., Australia, in 1953. He received the B.Sc. degree in physics from Deakin University, Burwood, Vic., in 1976, a Grad Dip Education from Hawthorn State College, Melbourne, Vic., in 1977, and the Ph.D. degree in otolaryngology from the University of Melbourne, Vic., in 1987, examining the safety and efficacy of cochlear implants.

He is currently the Director of the Bionics Institute, Melbourne, and a Professor of Medical Bionics, The University of Melbourne. His current research interests include the development of retinal prostheses and neural prostheses for neurological disorders, as well as contributing to improvements in cochlear implant design.

Prof. Shepherd is a Member of the Association for Research in Otolaryngology, Association for Research in Vision and Ophthalmology, the Australian Neuroscience Society, and is a Life Member of the International Functional Electrical Stimulation Society.